A New Look at Compact Groups in WISE Mid-Infrared

Natalie Butterfield and Allison H. Savage
Department of Physics and Astronomy, University of Iowa, Iowa City, Iowa 52242

ABSTRACT

Using WISE color-color data, we identify the morphology of 129 member galaxies within 33 compact groups. We present a systematic approach to identifying compact group members that are QSOs, ULIRGs, LINERs, starbursts, and LIRGs. Our results supplement and replace, in some cases, the classifications for these galaxies that are currently available in the literature. We compare the "canyon" region of Walker et al. (2012), which is a gap between gas-rich and gas-poor galaxies, with WISE color space. We do see a "canyon" region in WISE colors, but it is very narrow. Finally, we compare HI gas content within the 15 CG galaxies to the WISE colors, and we find a significant correlation between the two for Sequence A & B galaxies.

1. Introduction

Since our ability to observe the early universe is limited by distance, time, and technology, it is necessary to find similar environments in the local universe that can provide insights to the past. Compact groups (CGs) are thought to be one of these environments that share similar attributes with the early universe like having a high number density of galaxies and low velocity dispersions (Pompei & Iovino 2012). Hickson (1997) defines a CG as an isolated, small system of 4-5 galaxies in close proximity to one another. Such groups are not unbound, chance superpositions but dynamically bound systems (Barton et al. 1996; Hickson & Rood 1988; Mamon 1986). A number of studies have cataloged CGs (e.g. Hickson et al. (1992); Rose (1977); Barton et al. (1996)), and multiple studies have been conducted to determine properties of CGs. The two catalogs of interest for this paper are the Hickson Compact Groups (HCGs), which consists of 100 CGs, and the Redshift Survey Compact Groups (RSCG's) that contains 89 CGs (Barton et al. 1996). These catalogs will be discussed further in Section 2.1.

The morphology of CGs and the member galaxies within CGs have implications for cosmology. Galaxies within CGs have strong tidal interactions that impact their evolution (Barnes 1989), and they are dynamically dominated by dark matter and may be a potential environment in which to study dark matter (Hickson 1997). Rood & Williams (1989) found that CGs have a significantly smaller fraction of spirals and irregular type galaxies (late-type), and a given CG is more likely to host similar type (late or early) of galaxies than allowed in a random distribution and found in a random field sample of galaxies (Kindl 1990; Hickson 1997). Unlike the early universe, GCs have lower populations of spiral galaxies, which makes CGs very unique due to the strong tidal interactions. In some cases, the end result of CGs may be a merger of the galaxies into a bright, giant, elliptical galaxy (Barton et al. 1996; Barnes 1989; Carnevali et al. 1981; Cavaliere et al. 1983; Governato et al. 1991). Determining the morphology of group members may give insight into initial galaxy populations and the subsequent evolution of galaxies. The morphologies of CG members also correlate with characteristics of their host CG, like the velocity distributions of the galaxies. Higher velocity dispersions correlate to fewer late-type galaxies in CGs (Hickson 1997).

Determining the morphology of the members of CGs is difficult due to the interactions within the group. Arp (1973) studied the shapes of CGs and found that "chains" of galaxies were features of CGs. Hickson (1984) and Malykh & Orlov (1986) concluded a similar result from the study of the HCGs and confirmed that CGs were not random projections or chance crossings. If the CG galaxies were a collection of chance crossings, the interactions of the galaxies would strip any inherent ellipticity from the group (Hickson 1997) and the "chain" feature would not be observed. From multi-frequency studies, ranging from radio continuum to X-ray, the usual characteristics that have been used to identify late-type and early-type galaxies are insufficient. CGs usually lack neutral hydrogen compared to other loose groups, and interactions of galactic members have removed much of the gas from the galaxies, gas that would normally give indication in the HI line of spiral galaxies (Williams & Rood 1987; Menon 1995). Another property of CGs that makes morphological identification of the members difficult is that within the contained galaxies, the original gas has been distributed throughout the group, sometimes forming an envelope surrounding it (Hickson 1997). Previous X-ray observations have provided information about the hot gas in the clusters, including metalicity and temperature, but these studies indicate that the CG members have gas envelopes and dark matter halos, which would merge before the baryonic matter (Barnes 1984; Bode et al. 1993).

Studies with the Infrared Array Camera (IRAC) on Spitzer using polycylic aromatic hydrocarbon (PAH) emission, which traces warm dust and star formation, show that as CG galaxies transition from being gas-poor to gas-rich, the amount of PAH emission in the galaxies increases as well as the temperature of the dust (Walker et al. 2012). In Figure 1, CG galaxies from Walker et al. (2012) sample are plotted in IRAC color bands of [3.6]-[5.8] and [4.5]-[5.8], where the color of the markers represents gas-poor galaxies in blue, and gas-rich galaxies in red. As galaxies transition from gas-poor to gas-rich along the fitted line in Figure 1, there is an increase of PAH emission observed as well as an increase in dust temperature due to stars ionizing and heating the dust in the galaxy (Walker et al. 2010, 2012). Walker et al. (2012) suggests that galaxies within CGs contain varying distributions of dust that indicate whether a galaxy is forming stars (active) or quiescent.

From initial IRAC studies of CGs conducted by Johnson et al. (2007), a sparsely populated region between the gas-rich and gas-poor galaxies was found, which they termed the "gap" region and

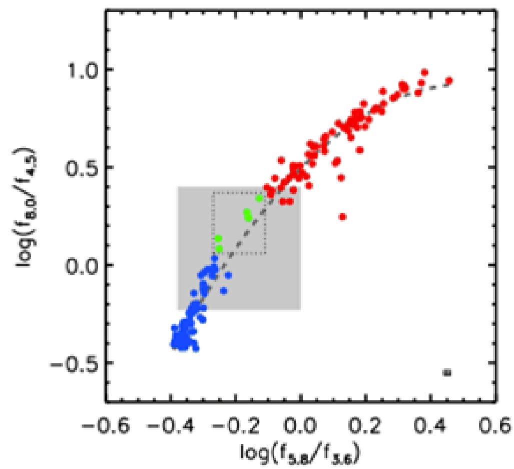

Fig. 1.— From Walker et al. (2012). A plot of the IRAC color bands of [3.6]-[5.8] and [4.5]-[8.0] shows the canyon region, which is outlined by the dashed box. The gray box shows the "gap" in Johnson et al. (2007), which has since been narrowed to the canyon by Walker et al. (2012). The colors of the markers represent gas-poor (blue) and gas-rich (red). The dashed line shows that the PAH emission eventually levels off, which indicates a limit for the PAH emission.

is shown in Figure 1 as the shaded gray portion of the graph. This "gap" region was also verified in independent studies performed by Tzanavaris et al. (2010), which looked at 11 GCs in the UV, and they found that there was also a gap in the specific star formation rate (SSFR), which traces young stars. Further studies were done by Walker et al. (2010) that looked at a comparison of both MIR and UV linear plots and found that the gap regions lined up. Walker et al. (2012) expanded the sample of 12 groups and found that the original gap was better described as a "canyon" region that had low number densities relative to the gas-rich and gas-poor groups. For the CG galaxies in the Walker et al. (2010) survey, the "canyon" region is defined to be where the number of galaxies is less than half of the average number of galaxies (See Figure 2). This under density in population suggests a short time scale to evolve from gas-rich to a gas-poor galaxy. The "canyon" region is seemingly unique for CGs as this relationship is not observed for other environments, such as loose groups and interacting pairs. Using the Kolmogorov-Smirnov test, Walker et al. (2010)

modeled a cumulative distribution of the color-color curve for galaxy densities in four distinct environments in order to test whether or not the canyon region was unique to the CG environment. These environments include interacting pairs, the Coma center, the Coma infall, and LVL+SINGS (See Figure 7 in Walker et al. (2010)), and models of these environments do not reproduce the canyon region.

Since the canyon galaxies represent a brief period in a galaxy's evolution, a survey was done using the g', r', and i' data from the Sloan Digital Sky Survey (SDSS) (dr 8 edition) (Butterfield et al. in progress). They wanted to investigate if the canyon galaxies also fell in the green valley on the color-magnitude diagram (CMD). The green valley is the region that lies in between the red sequence and the blue cloud Gaussian peaks, where the blue cloud is thought to be composed of spirals, and the red sequence is mainly ellipticals (Hogg et al. 2004; Smolčić 2009). The green valley is also thought to be a transition region delineating when a galaxy has recently ended star formation (Smolčić 2009). As the young blue stars die off, the ratio of blue light to red light will decrease, and the galaxy will pass through the green valley into the red sequence.

Despite the similar environment to the early universe, Butterfield et al. (in progress) found that the majority of the CG galaxies fell in the red sequence. This was unexpected since the early universe had a much higher number density of spiral galaxies. Butterfield et al. (in progress) compared their findings with the Walker et al. (2012) MIR data and found that while the blue MIR galaxies were mainly condensed in the red sequence, the red MIR had a large spread through the optical colors. This indicates that there is dust obscuring the blue light of galaxies in the red sequence. Since lenticular galaxies are found in the red sequence and spirals in the blue cloud, this gives a false impression that many of these CG galaxies are ellipticals. Constraining the morphology within these bands would give better estimates of galaxy morphology distributions in CGs, which may also give insight into distributions of the early universe.

Currently, the identification of galaxies is compiled from the literature in the NASA/IPAC Extragalacitc Database (NED), which offers an *a priori* look into the morphologies of the galaxies within GCs. Figure 3 shows CG galaxies on a plot of optical colors vs. mid-infrared colors (henceforth referred to as "optmir plot"), where the x-axis corresponds to the distance along the

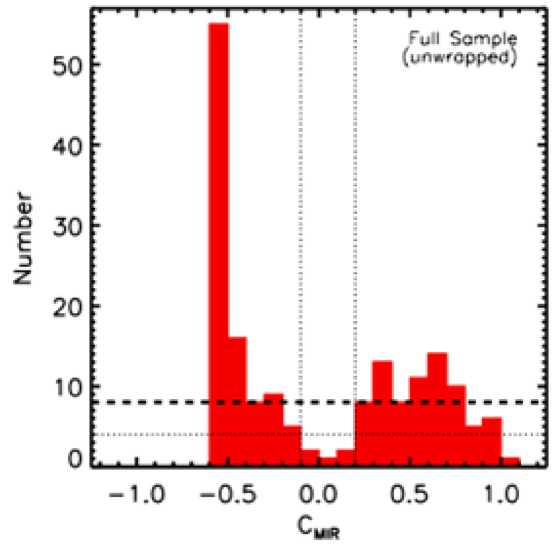

Fig. 2.— From Walker et al. (2010). Histogram of the number of galaxies v.s. the change in MIR color (ΔMIR). The bold dashed line is the average number of galaxies, and the normal dashed lines define the "canyon" region as less than half of the average number of galaxies.

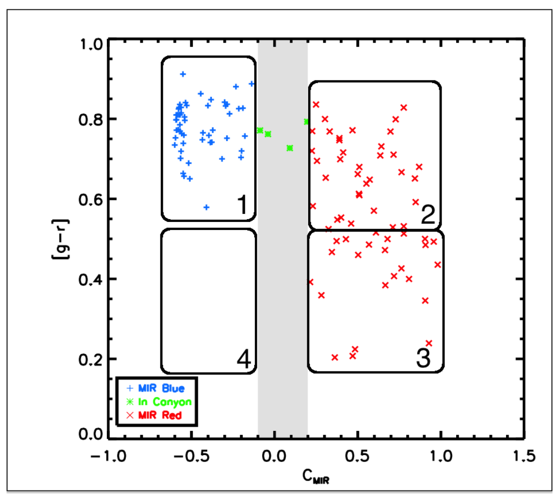

Fig. 3.— Color-color plot of optical vs MIR colors for CG member galaxies from the HCG and RSCG catalogs (Butterfield et al. in progress). Four areas shown correlate dust and star formation. The regions are further described in the text.

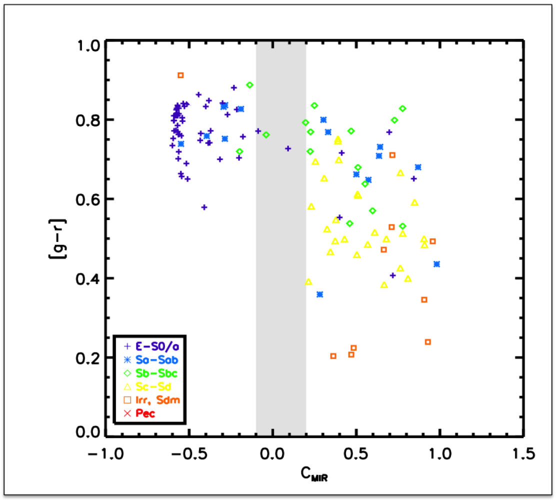

Fig. 4.— The same plot as Figure 3 except that the galaxies have their morphologies indicated, which were complied by NED.

line of best fit (dotted line) in Figure 1. This illustrates an"unwrapping" of the best fit line to show a clear separation between the gas-rich and gas-poor galaxies. Figure 4 shows the optmir plot with symbols indicating the morphology of galaxies as classified in NED. The optmir plot has four main areas of interest for star formation, shown in Figure 3:

1. Galaxies with cold dust and no current star formation are blue in MIR and red in optical- the "red and dead" galaxies,
2. Dust obscured galaxies with warm dust and current star formation are red in both MIR and optical,
3. Galaxies with warm dust, young stars, and current star formation are red in MIR and blue in optical,
4. Galaxies with young stars but no current star formation are blue in both bands, which indicates that star formation has recently ended.

NED is an incomplete compilation of morphologies for many CG galaxies, and for the CG members it does identify, there are few variations beyond spirals and ellipticals. Two opposing questions can be drawn from current identifications: 1) How are CG members overwhelmingly spirals and elliptical galaxies in such environments with strong tidal forces, mergers, and intense interactions or 2) If CG members are not just spiral and elliptical galaxies, what does the morphology say about star formation and dust content within CGs? We expect the later, but in order to answer either of these questions, we will determine morphology for CG members.

Once we determine the morphology for CG galaxies, we will also investigate star formation and dust content of these galaxies using HI maps from previous studies of CGs conducted by Verdes-Montenegro et al. (2000) and Verdes-Montenegro et al. (2001). Studies of HI content by Johnson et al. (2007) and Konstantopoulos et al. (2010) indentified two different kinds of CGs, Sequence A and Sequence B, which are defined by the compactness of the HI gas in CG galaxies. In Sequence A, the gas is mostly contained within the member galaxies, and the individual galaxy's star formation is uninterrupted as the gas is consumed before any major galaxy interactions can occur within the group. The gas does not play a role in the eventual "dry merger" into an elliptical galaxy. In Sequence B, the gas is spread throughout the Intergalactic Medium (IGM), and multiple strong interactions can occur between the galaxies throughout the group's evolution, which can strongly affects star formation rates.

Previous to the Sequence A and B classification, Verdes-Montenegro et al. (2001) had categorized the CGs into an "evolutionary sequence" of three scenarios based on the HI gas content and distribution in the galaxies, which are Type I) galaxies pre-interaction, Type II) a shocked intergroup medium of HI gas, and Type III) a smooth intergroup medium of HI gas (See Figure 1 of Konstantopoulos et al. (2010)). Johnson et al. (2007) adopted the three evolutionary scenarios and quantified them as I) relatively HI rich, $\log(M_{HI})/\log(M_{dyn}) \geq 0.9$, II) intermediate HI, $0.9 > \log(M_{HI})/\log(M_{dyn}) \geq 0.8$, and III) relatively HI poor, $\log(M_{HI})/\log(M_{dyn}) < 0.8$, where the M_{HI} and M_{dyn} have been normalized by $M_{\odot}$. Previous studies of the evolutionary sequence done by Johnson et al. (2007) and Konstantopoulos et al. (2010) were limited in the number of CGs, 12 and 1, respectively. In this paper, we will expand the number of CGs to 33.

In 2010, the Wide-field Infrared Survey Explorer (WISE) completed a MIR survey of the entire sky. WISE offers high sensitivity in 4 IR bands, 3.4, 4.6, 12, and 22μm (Wright et al. 2010). Previous studies in the MIR using IRAC on Spitzer did not offer the all sky coverage of

WISE, and IRAC bands cover only a fraction of the frequency range that WISE does. The completion of WISE provides new opportunities in the MIR to identify morphologies of CG galaxies in order to understand star formation and dust content in the turbulent environments of CGs. Our sample of 33 CGs will provide an in-depth analysis of the "evolutionary sequence" proposed by Verdes-Montenegro et al. (2001), and we will investigate the "canyon" region in the WISE colors in order to compare it to the Walker et al. (2012) region.

2. DATA

2.1. Selection of Compact Groups

The 33 CGs chosen for this project are from the Hickson Compact Group catalog (HCG; Hickson (1982)) and the Redshift Survey Compact Group catalog (RSCG; Barton et al. (1996)). Due to the nature of selection criteria of the two different catalogs, we will briefly summarize the original criteria. The HCG catalog selected CGs from the Palomar Sky Survey, requiring at least 3 galaxies within 3 magnitudes of the brightest galaxy; isolation of the group from external galaxies within a certain magnitude range; and compactness, requiring the surface brightness averaged over the smallest circle containing the galaxies to be $\bar{\mu}\leq 26.0/$ mag arcsec^{-2} (Hickson 1982). The RSCG catalog utilized a magnitude-limited redshift survey to identify CGs and their members and was created to have similar properties to the HCG catalog (Barton et al. 1996). From the HCG and RSCG catalogs, we selected CGs that have IRAC and SDSS data available, and we used a redshift criteria of $z\leq 0.035$ as well. IRAC and SDSS data enables us to analyze HI properties and compare possible correlations in optmir color to morphology. Table 2 lists the CGs and the member galaxies selected from the HCG and RSCG catalog.

2.2. Procedure

For each member galaxy in the CGs, we obtained infrared data from the WISE point source catalog. Comparing the sources to SDSS, we determined that the cores of the galaxies are point sources in WISE. The average angular size of the galaxies was 20 arcsecs ("), with a maximum of 2 arcmins, which is much larger than the WISE resolution of 6.1" and 12". We adopt a point source approach to the relative centers of the sources and do not integrate over the size of the galaxies. We do this because there are two problems when determining the spatial extent of the galaxies: (1) galaxies within CGs experience strong tidal forces that may strip gas, dust, and stars from the galaxies and deposit or stretch said contents outside of the initial diameter of the galaxy, (2) pairs of galaxies may merge on smaller timescales than the timescale for the CG as a whole to merge. Figure 5 shows HCG 56, a compact group with five member galaxies, which illustrates situations (1) and (2) in tandem.

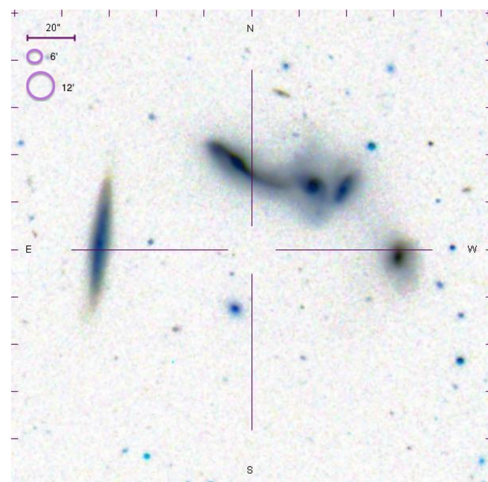

Fig. 5.— SDSS image of HCG 56 illustrating two potential problems when determining the spatial extent of galaxies in environments of strong tidal forces and mergers. The SDSS resolution is 20", and the two WISE angular resolutions are the circles of $\sim$ 6.1" and $\sim$ 12".

With the WISE data, we produced color-color plots of the magnitudes of 3.4, 4.6, and 12 μm. The 3.4, 4.6 and 12 μm bands correspond to the WISE colors of w1, w2, and w3, respectively. The color-color plots were constructed by taking the difference in magnitudes in the 3.4 and 4.6 μm bands and plotting it against the difference in magnitudes of the 4.6 and 12 μm bands,

$$\frac{[3.4]-[4.6]}{[4.6]-[12]}$$

Using the regions colored on Figure 6, we identified the types of galaxies in the CGs.

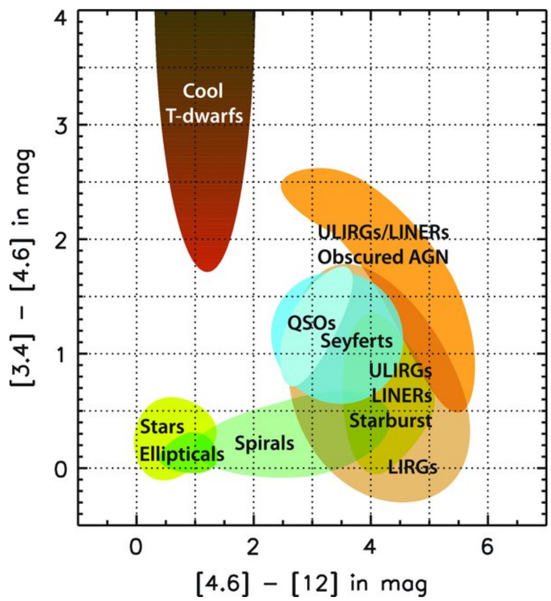

Fig. 6.— Color-color diagram of WISE data showing locations on the plot of type of galaxies. This diagram is from Wright et al. (2010), Figure 12.

The regions we include in our classification system are as follows: Stars, Elliptical, Spirals, Spiral/LIRG[1], Starburst, LIRG, ULIRG/LINER[2], Seyfert, QSO[3], ULIRG/LINER Obscured AGN[4], and Cool T-dwarfs, all of which correspond to colors on Figure 6. One region that requires more explanation is the Spiral/LIRG. We include this region due to the lack of clarity in defining the regions provided by Wright et al. (2010).

3. Results

The results of our WISE color-color plots for each CG are shown in Figures 13 & 14 for the RSCGs and the HCGs respectively, and the identification of the galaxies is in Table 2. The identifications from this paper, which are presented in Table 2 column 10, correspond to regions on the WISE color-color diagram in Figure 6. The errors for each CG member were taken into account thus some galaxies have multiple classifications, and we list the CG members that have no classification based on the WISE diagram. In Table 2, we show the classification of the CG members complied from NED in column 5 for comparison with our identification. We discuss this more in Section 4.1.

Using the classifications of the galaxies determined from the WISE data, we constructed a histogram of the number of galaxies vs. the difference in the WISE colors, 4.6 and 12 μm (see Figure 7). We identified the canyon region for our sample of galaxies using the same criteria as Walker et al. (2010), who determined the canyon region to be where the number of galaxies fell to half of the average number. In the WISE colors, our canyon is between $2.1 \leq [[4.6]\text{-}[12]] \leq 2.7$ in magnitude, which lies in the spiral region of Figure 6.

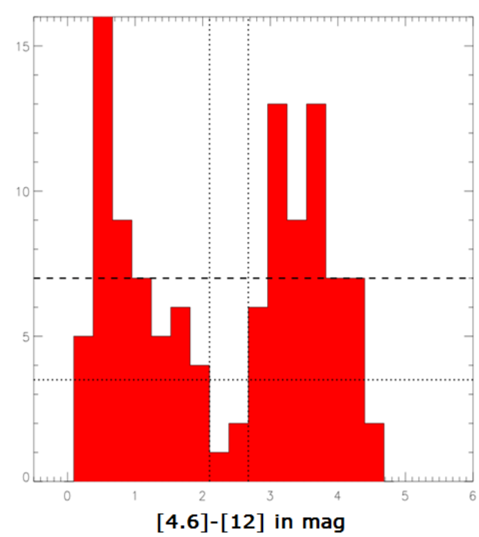

Fig. 7.— A histogram of the number of galaxies vs. the WISE colors of 4.6 and 12 μm. This histogram reflects the galaxies as classified by this paper and shows the associated canyon region.

3.1. Errors

The errors on the positions are listed in Table 2, however they are relatively small. Two galaxies had large errors, and they were both classified as LIRGS. Large errors may be a result of using a point source catalog for particular galaxies that are not strictly point sources to WISE. Galaxies not identified are mainly due to the member galaxies being to close in angular projection for WISE

[1]Luminous infrared galaxy (LIRG)

[2]Ultra luminous infrared galaxy (ULIRG); Low-ionization nuclear emission-line region (LINER)

[3]Quasi stellar object (QSO)

[4]Active galactic nuclei (AGN)

to distinguish two sources. Other factors during the observation could also affect the quality of the data.

4. Discussion

4.1. Classification

We classified 129 galaxies within 33 CGs; two galaxies are classified as QSOs and two are Seyferts. Figure 8 is a complied graph of all the identified galaxies. NED offers galaxy classification through literature searches, however the current classifications for our galaxies are primarily available from the de Vaucouleurs et al. (1991) catalog, which expanded upon the Hubble system. de Vaucouleurs et al. (1991) visually inspected the optical images of galaxies in order to classify them. This approach is not systematic and is biased towards the classifier. Identifying galaxies based solely on optical data precludes possible identification of such types like LINERs, ULIRGs, QSOs, Starbursts, and LIRGs. NED is also not complete in its classifications as many galaxies are not yet classified, and many galaxies have multiple classifications from multiple papers. Our classification is systematic, unbiased, and can identify galaxies beyond ellipticals and spirals, within errors. Specifically, we have established a process that can identify QSOs and Seyfert galaxies that are not detected in optical bands.

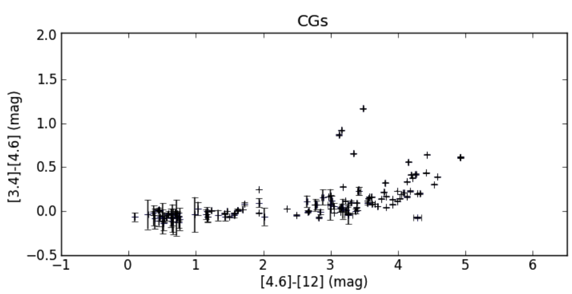

Fig. 8.— WISE color-color plot of the 129 galaxies surveyed.

4.2. The Canyon Region

Similar to the Johnson et al. (2007) and Walker et al. (2010) studies, we found a canyon region in the distribution of galaxies in the WISE colors. However, the canyon from this study is much narrower than that of Walker et al. (2012), and our canyon region contains three galaxies, HCG 79B, HCG 47A, and HCG 47D. To investigate possible correlations between the two canyon regions, we designated the colors of the galaxies to reflect the IRAC colors in Figure 9, using blue for galaxies containing cold dust, green for canyon galaxies, and red for galaxies with warm dust, which correspond to the colors in Figure 1. Comparing the IRAC and WISE bands, it is evident that there is not a one-to-one mapping for some galaxies. In our canyon region, HCG 79B is the only galaxy that is also contained in the canyon region of Walker et al. (2010). In the Walker et al. (2010) canyon, HCG 47A and HCG 47D were listed as MIR red. Since there is not a one-to-one mapping of the canyon galaxies, this suggests that the galaxies were under sampled. A larger survey in both WISE and IRAC colors would narrow the canyon further because the canyon region is defined to be where the density of galaxies is half of the median galaxy density. We can "fine-tune" the canyon region by enlarging our survey to include more galaxies, which would only further constrain the canyon region. From the definition of the canyon, increasing the sample size would not remove the region. Another example of the discrepancy between the IRAC and WISE bands is RSCG 66B. In IRAC colors, RSCG 66B falls in the warm dust region, but in WISE colors, it falls with the cold galaxies. This discrepancy could indicate that the galaxy is in transition between having active star formation and becoming quiescent.

As discussed in the Introduction and in Figure 3, the regions surrounding the canyon indicate star formation and dust quantities within the galaxies. The canyon region is thought to be a transition region in which galaxies are changing from having active star formation to becoming inactive, or vice versa. It is possible for the galaxies within CGs to transition between these regions because mergers and interactions create strong tidal forces, which change the gas distribution within the galaxies. Since our canyon falls in the spiral region of the WISE bands, this could constrain star formation activity within spirals, being either an active or inactive spiral galaxy.

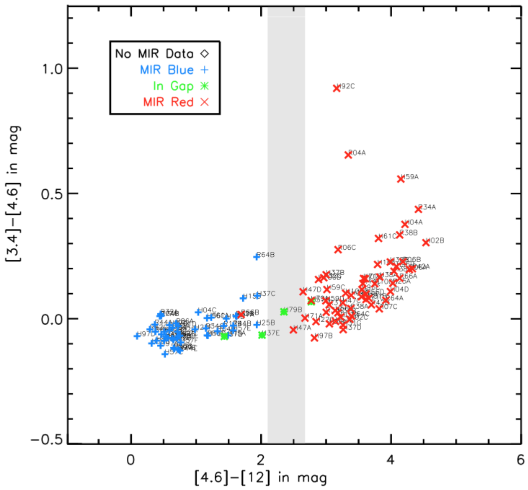

Fig. 9.— A plot of the WISE color bands with the sources colored in IRAC colors. Some sources from our sample are not present due to the sources not being apart of the Walker et al. (2010) IRAC survey. This difference is noted most obviously in the QSO and Seyfert region of the graph.

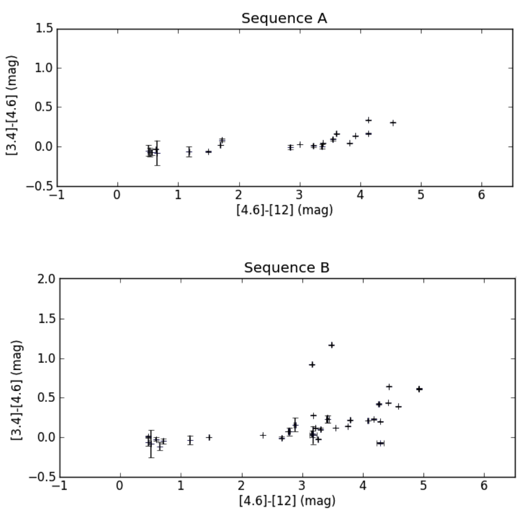

Fig. 10.— WISE color-colors plots of Sequence A and B.

4.3. Distribution of HI in CGs

Johnson et al. (2007), Konstantopoulos et al. (2010), and Verdes-Montenegro et al. (2001) categorized CGs into two sequences, Sequence A and Sequence B, and then further divided the CGs into three evolutionary scenarios, Type I (HI-rich), Type II (intermediate HI), and Type III (HI-poor). Though previous studies identified the Sequences and Types of some galaxies in CGs, the samples were small. From our sample, 15 out of 33 CGs had sufficient HI data available. The two sequences are plotted in the WISE colors in Figures 10(a) & 10(b), and in Table 1, we report sequence and type.

Table 1: Summary of Sequence A and B CGs and the Type I (HI-rich), II (intermediate HI), and III (HI-poor).

Sequence A	Sequence B
Type I	
HCG 2	HCG 16
	HCG 31
	HCG 54
Type II	
HCG 7	HCG 96
RSCG 38	HCG 100
RSCG 66	HCG 79
	HCG 92
	RSCG 6
	RSCG 34
Type III	
HCG 15	
HCG 22	

By comparing the WISE color plot and the HI maps of the CGs, for Sequence A, we determined that the [4.6]-[12] color magnitude decreases as the HI in the gas is depleted in the galaxy. Galaxies within Type I CGs are on the right of the "canyon", indicating an excess of HI in the group and very active galaxies. Type III fall on the extreme left of the canyon near the elliptical galaxies, with one exception, HCH 15F, which is located with the Type I galaxies. Looking at the HI map of this group, HGC 15F hosts HI, unlike the other members of HCG 15. Type II galaxies are distributed throughout the [4.6]-[12] colors. When looking at the individual galaxies in Type II, we see that the galaxies containing HI are located to the right of the canyon region, which indicates active starformation. The CG galaxies lacking in HI, or where the HI is distributed in the Intergalactic Medium, are located to the left of the canyon region and are quiescent galaxies.

Looking at Sequence B, we do not see an even distribution of galaxies in the [3.4]-[4.6] band; there are more galaxies to the right of the canyon region in the active star forming section. The

Type I CG galaxies generally are located to the right of the canyon region; the exceptions are HCG 16B and HCG 54A. The Type II CG galaxies are distributed on either side of the canyon region. In Sequence B, there are two galaxies that are distinguished from the general distribution of galaxies, HCG 92C and HCG 96A, both of which are QSOs. Only Sequence B has the QSO galaxies, but we believe this to be a selection bias as we only have 15 CGs available. We did not have any CGs that met the Type III requirements.

Type I CG galaxies in both sequences tend to fall to the right of the canyon, Type II galaxies are distributed on either side of the canyon, and Type III members are located predominately to the left of the canyon. The exceptions to the Type I and III trends indicate that galaxies, regardless of Type (I, II, or III), which have HI still tied to the galaxies fall to the right of the canyon region, in the active star forming section, but galaxies lacking in HI are to the left of the canyon region, the quiescent, inactive star forming side. In the future, it may be beneficial to classify the galaxies as Type I, II, or III to analyze the interactions and mergers in the CGs. From examining the HI maps and the WISE morphology of the galaxies, we do see that there is a correlation between the two. HI-rich galaxies tend are to the right of the canyon region and are active galaxies like starbursts, ULIRGS/LINERs, LIRGS, and QSOs. HI-poor galaxies are quiescent ellipticals and spirals and are to the left of the canyon region.

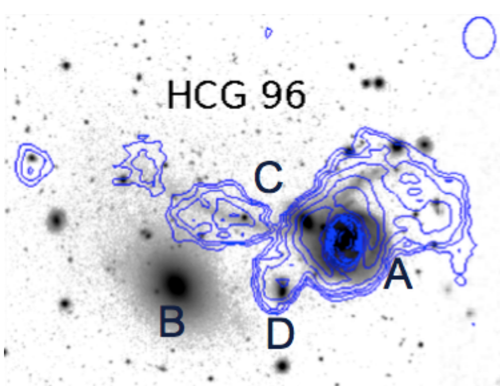

Fig. 11.— Plot for HCG 96 with HI contours, which represent the HI content within the galaxies (Verdes-Montenegro et al. 2000).

A specific example is HCG 96, which is a Sequence B, Type II group. Looking at the distribution of HI around the group (Figure 11), there is a high concentration of HI around Galaxy A and diffuse gas extending out into Galaxy C and Galaxy D. In Figure 11, Galaxy B appears to be void of HI, relative to the other group members. Then, we compared the HI contour maps with the classification based on the WISE morphology (Figure 12), and we see that HI does play a clear role in the evolution of the group and the morphology of the individual galaxies. Since ellipticals are believed to form from galaxy mergers (Barton et al. 1996; Konstantopoulos et al. 2010), Galaxy B might be from a previous merger in the group's lifetime, which consumed the HI in star formation and left behind an elliptical galaxy.

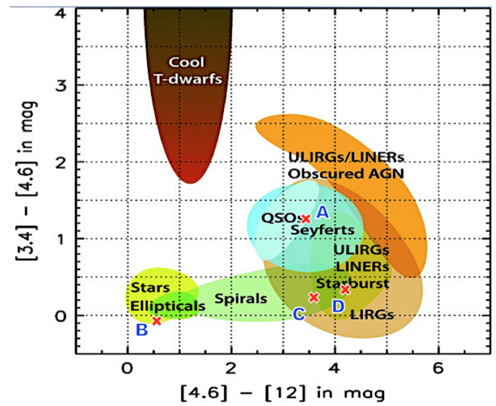

Fig. 12.— A WISE color-color plot for HCG 96 overlaid on the WISE morphology plot.

5. Summary

The conclusions of this paper are as follows:

- We classified 129 galaxies within 33 compact groups using WISE color-color diagrams. We identified 2 previously unknown QSOs and 2 Seyfert galaxies along with numerous starbursts, ULIRGS, LIRGS, and LINERS. Our classification system using the WISE color bands is a systematic process for identifying galaxies.
- We locate the canyon region for our galaxies and find only one galaxy, HCG 79, which is consistently in the canyon regions of Johnson et al. (2007) and Walker et al. (2010). Our canyon region is narrower than previous

studies, and we suggest that the canyon region should be narrowed. The canyon region could indicate a transition region between active star forming and inactive galaxies for CG members.

- We find a significant correlation between the degree of which the HI gas is bound to the host galaxy and the galaxy's position on the WISE color-color diagram. Galaxies with bound HI gas are active galaxies like starbursts, ULIRGS/LINERS, LIRGS, and QSOs, whereas galaxies lacking in HI tend to be elliptical and inactive spiral galaxies.

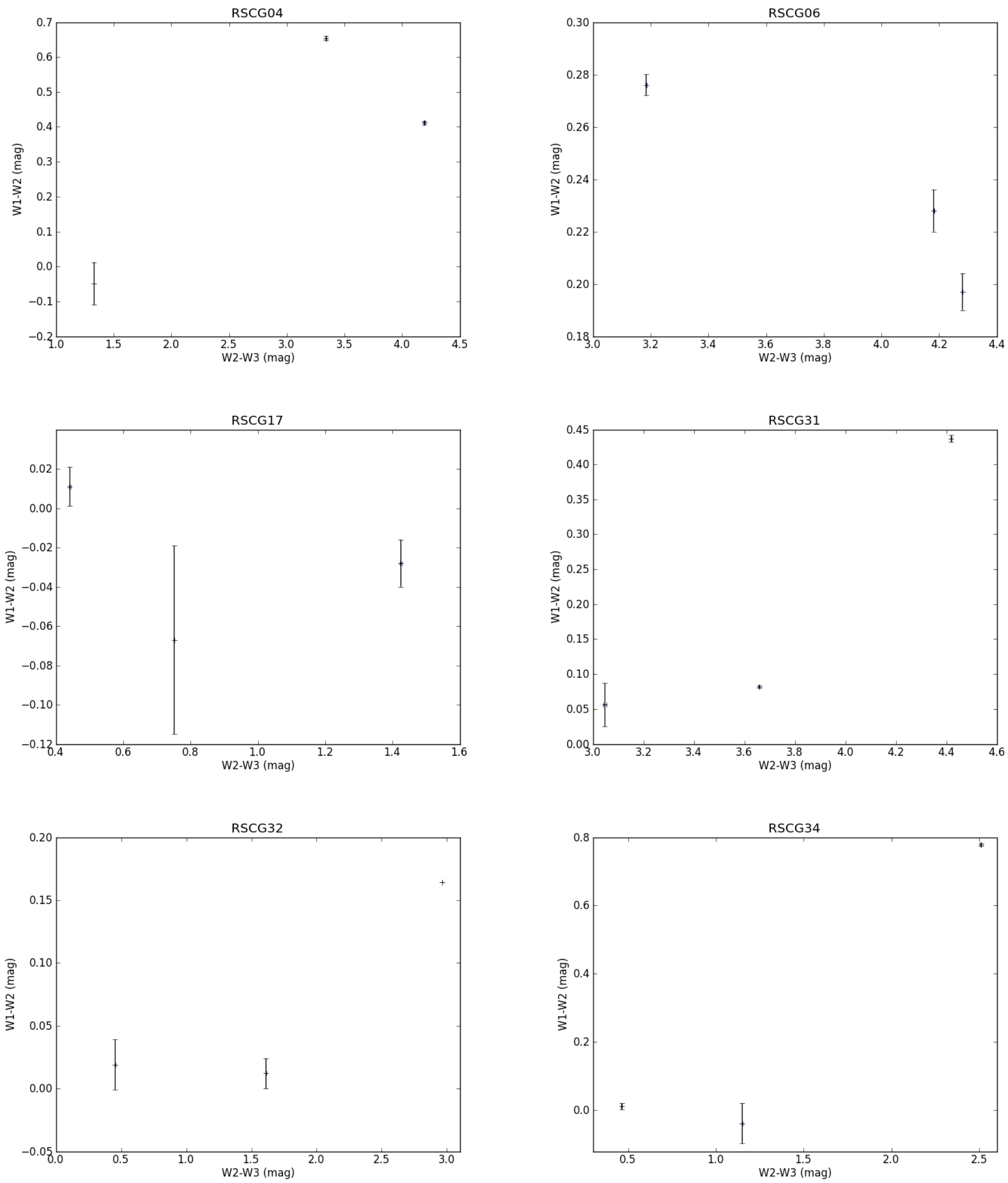

Fig. 13.— Color-color map of WISE data for CG members from the RSCG catalog. Plotted on the x-axis is the difference in magnitudes of 4.6 and 12 μm and on the y-axis is the difference in magnitudes of 3.4 and 4.6 μm. Figure continues...

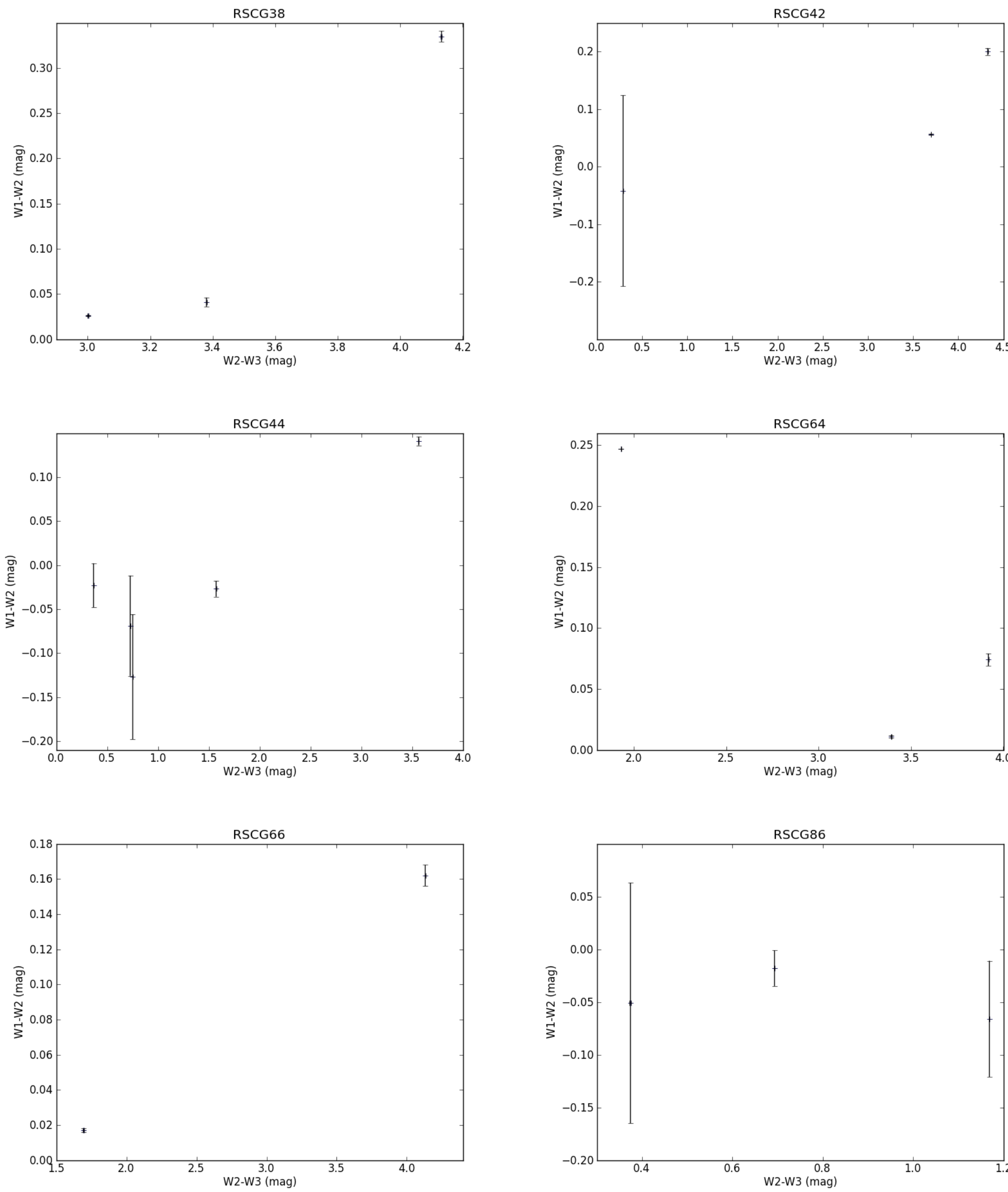

Figure 13 (continued)

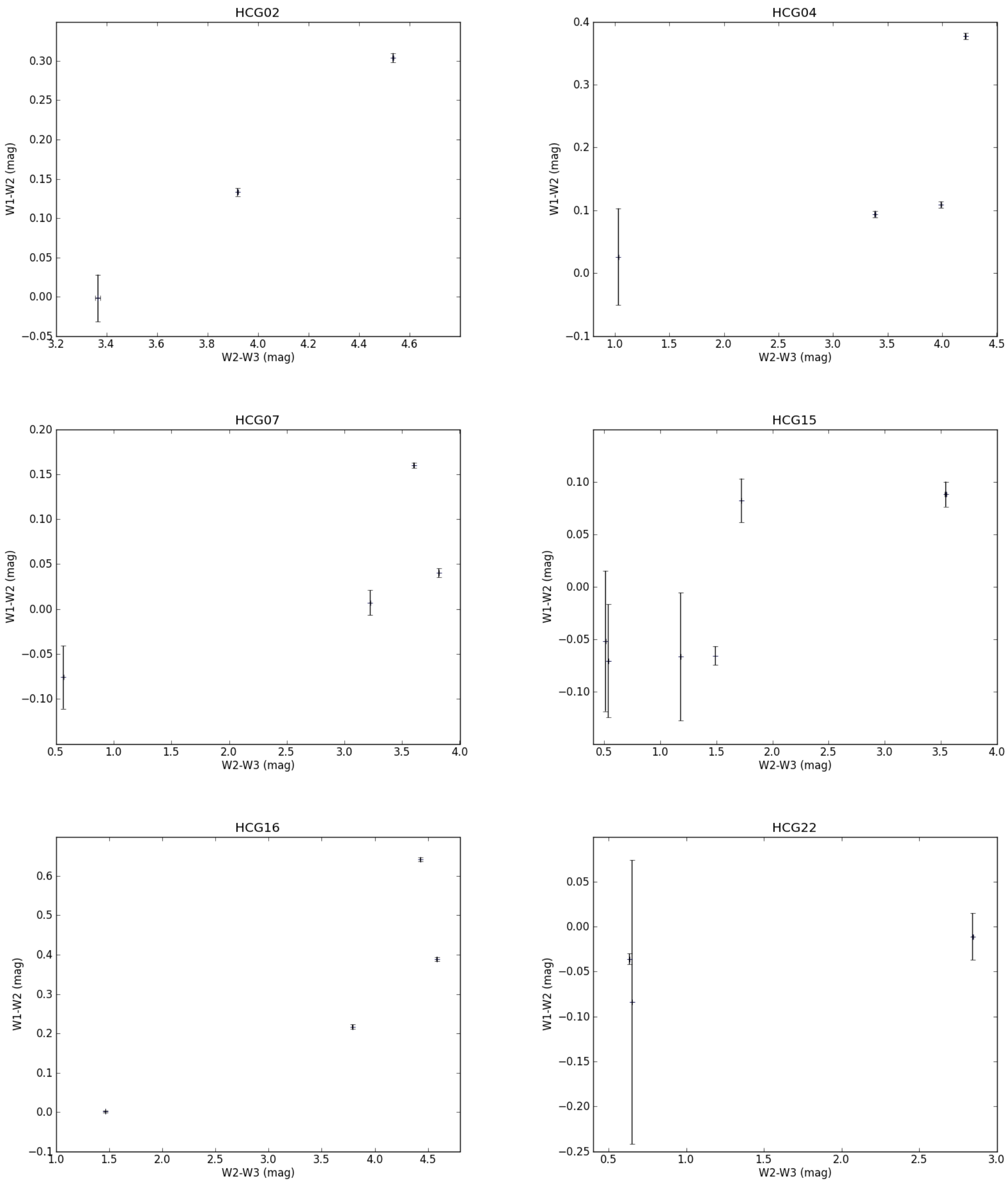

Fig. 14.— Same as Figure 13 except plotted are the CG members of the HCG catalog. Figure continues...

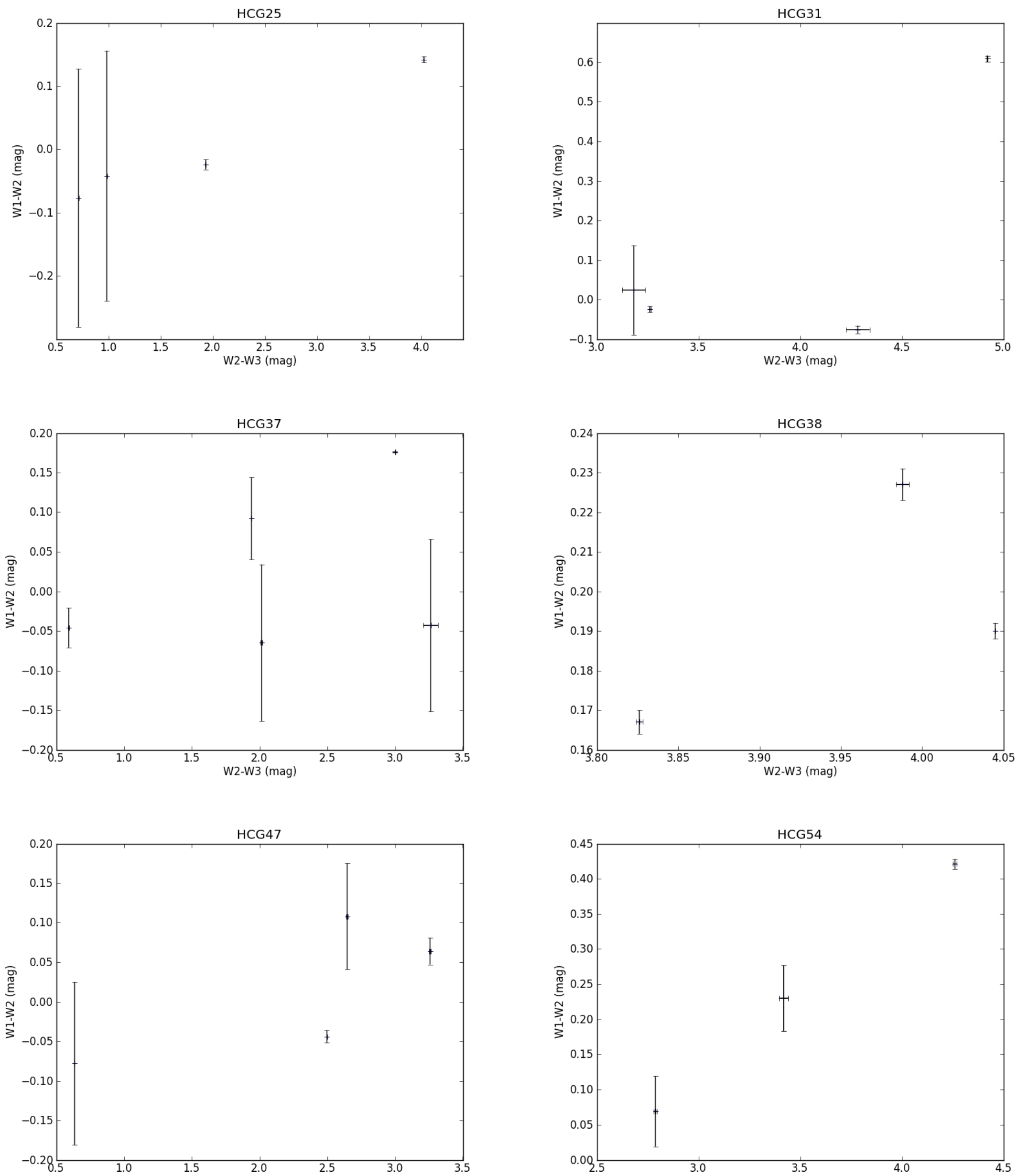

Figure 14 (continued)

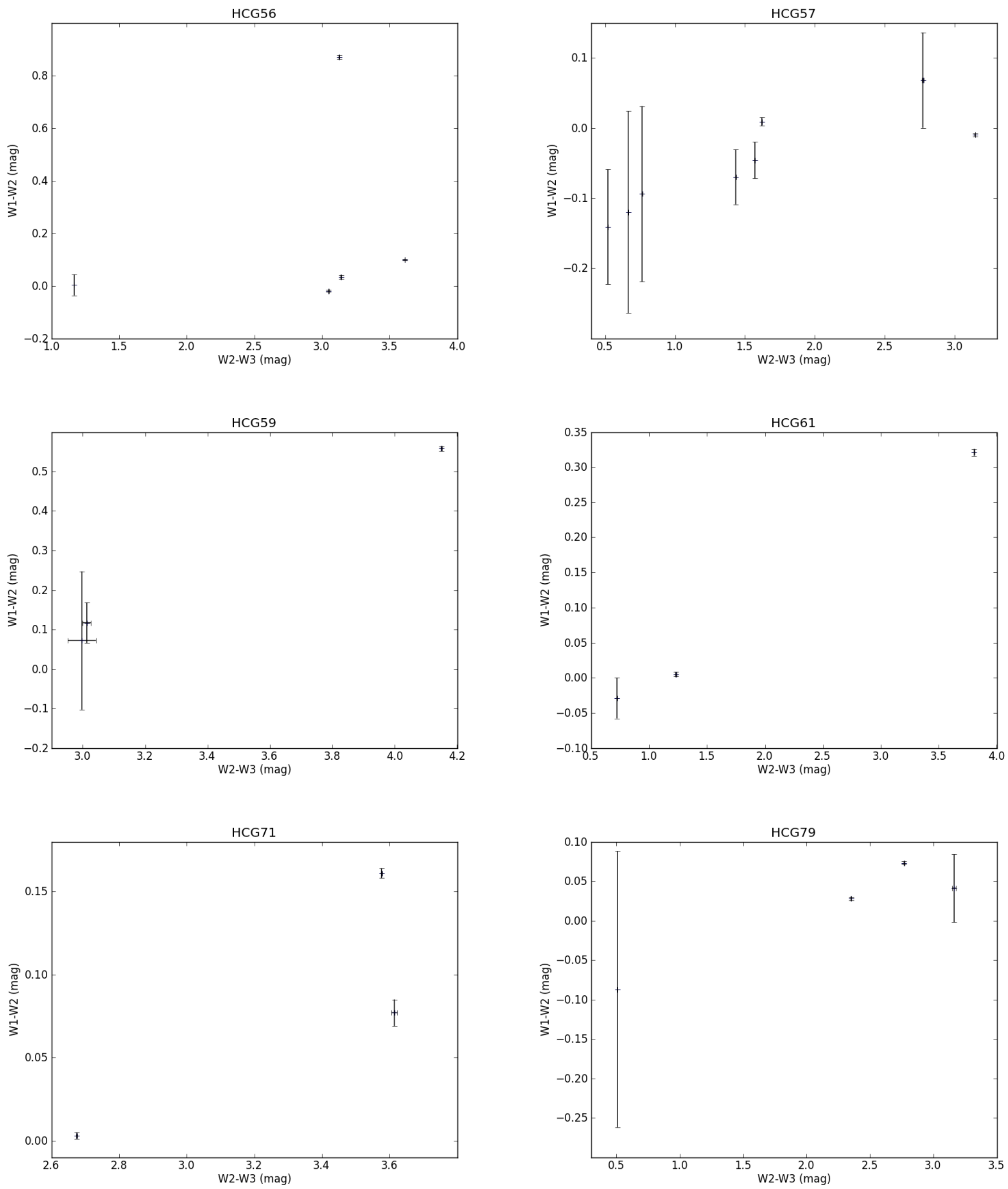

Figure 14 (continued)

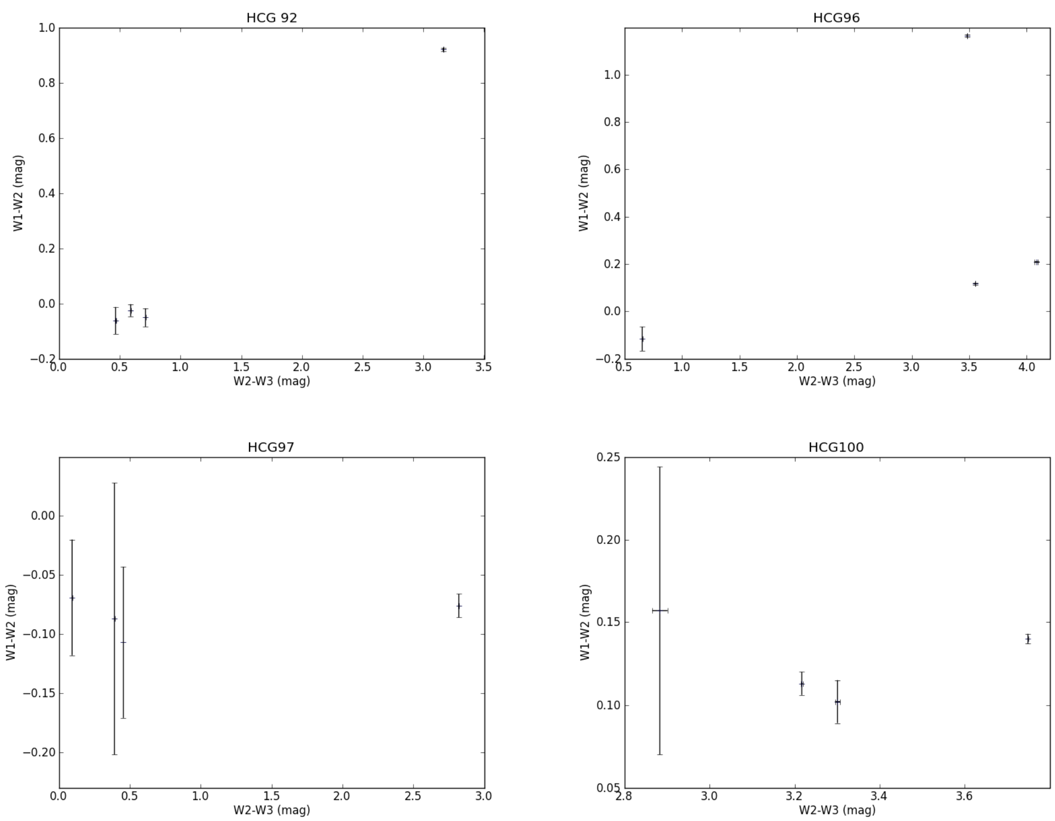

Figure 14 (continued)

TABLE 2

SOURCE LIST OF CGS AND THE MEMBER GALAXIES CHOSEN FROM THE HCG AND RSCG CATALOGS.

Member ID[a]	Galaxy Name	RA(J2000)	Dec (J2000)	NED Classification[b]	w2-w3[c]	σ_{w2-w3}	w1-w2[d]	σ_{w1-w2}	Classification[e]
				RSCG 4					
GalA	NGC 235A	00h42m52.8s	-23d32m28s	S0[f] ; Seyfert 1[g]	3.341	0.003	0.654	0.006	Sy
GalB	NGC 235B	00h42m53.6s	-23d32m44s	E0[f]	1.330	0.0009	-0.049	-0.061	E; x
GalC	NGC 232	00h42m45.8s	-23d33m41s	SD[f]	4.192	0.005	0.411	0.004	STB
				RSCG 6					
GalA	UGC 00816	01h16m20.5s	+46d44m53s	S[f]	4.281	0.001	0.197	0.007	U/L
GalB	UGC 00813	01h16m16.4s	+46d44m25s	Sb[m]	4.181	0.002	0.228	0.008	U/L
GalC	CGCG 551-011	01h16m04.5s	+46d43m50s	N/A	3.186	0.002	0.276	0.004	Sp/L
				RSCG 17					
GalA	NGC 0741	01h56m21.0s	+05d37m44s	E0[f]	0.441	0.002	0.011	0.01	E; St
GalB	NGC 0742	01h56m24.2s	+05d37m36s	E0[f]	1.425	0.003	-0.028	0.012	Sp; x
GalC	ARK 066	01h56m19.0s	+05d39m08s	compact[n]	0.751	0.0009	-0.067	0.048	E; x
				RSCG 31					
GalA	NGC 2798	09h17m22.9s	+41d59m59s	SB[f]	4.420	0.002	0.437	0.005	U/L
GalB	NGC 2799	09h17m31.0s	+41d59m39s	SB[f]	3.658	0.0009	0.082	0.002	L
GalC	UGC 04904	09h17m21.9s	+41d54m38s	SB[o]	3.047	0.007	0.056	0.031	Sp; x
				RSCG 32					
GalA	NGC 2832	09h19m46.8s	+33d44m59s	cD2[f]	0.454	0.002	0.019	0.02	St
GalB	NGC 2830	09h19m41.4s	+33d44m17s	SB0[f]	2.964	0.0009	0.164	0.0009	Sp
GalC	NGC 2831	09h19m45.5s	+33d44m42s	E0[f]	1.612	0.002	0.012	0.012	Sp
				RSCG 34					
GalA	NGC 2964	09h42m54.2s	+31d50m50s	SAB[f]	4.310	0.002	0.498	0.004	U/L;STB
GalB	NGC 2968	09h43m12.0s	+31d55m43s	Irr0[f]	0.463	0.003	0.012	0.009	E
GalC	NGC 2970	09h43m31.0s	+31d58m37s	E1[f]	1.150	0.001	-0.038	0.059	E; x
				RSCG 38					
GalA	NGC 3430	52:11.4	+32:57:01.53	SAB[f]	3.380	0.001	0.041	0.005	Sp/L
GalB	NGC 3424	51:46.9	+32:53:56.77	SB[f]	4.132	0.002	0.335	0.006	STB
GalC	NGC 3413	10:51:21	+32:45:49.02	S0[f]	3.001	0.002	0.026	0.001	Sp
				RSCG 42					

TABLE 2—*Continued*

Member ID[a]	Galaxy Name	RA(J2000)	Dec (J2000)	NED Classification[b]	w2-w3[c]	σ_{w2-w3}	w1-w2[d]	σ_{w1-w2}	Classification[e]
GalA	UGC 06583	11h36m54.4s	+19d58m15s	peculiar[f]	4.327	0.003	0.200	0.006	U/L
GalB	KUG 1134+202A	11h36m54.2s	+19d59m50s	S[f]	3.697	0.002	0.056	0.001	Sp/L
GalC	ARK 303	11h36m51.5s	+20d00m18s	high surface brightness galaxy[p]	0.289	0.001	-0.042	0.166	St
				RSCG 44					
GalA	NGC 3842	11h44m02.1s	+19d56m59s	E[f]	0.365	0.003	-0.023	0.025	St
GalB	UGC 06697	11h43m49.1s	+19d58m06s	Im[f]	3.566	0.001	0.141	0.005	Sp/L
GalC	NGC 3837	11h43m56.4s	+19d53m40s	E[f]	1.572	0.003	-0.027	0.009	Sp
GalD	NGC 3845	11h44m05.4s	+19d59m46s	S[f]	0.001	-0.127	0.071	St; x	0.751
GalE	NGC 3841	11h44m02.1s	+19d58m19s	S[f]	0.726	0.001	-0.069	0.057	E; St; x
				RSCG 64					
GalA	NGC 4615	12h41m37.3s	+26d04m22s	Scd[f]	3.919	0.001	0.074	0.005	U/L
GalB	NGC 4614	12h41m31.5s	+26d02m34s	SB0[f]	1.931	0.002	0.247	0.0009	Sp
GalC	NGC 4613	12h41m28.9s	+26d05m19s	Sa[m]	3.393	0.001	0.011	0.001	Sp/L
				RSCG 66					
GalA	NGC 4654	12h43m56.6s	+13d07m36s	SAB[f]	4.132	0.002	0.162	0.006	STB; U/L
GalB	NGC 4639	12h42m52.4s	+13d15m27s	SAB[f]	1.693	0.003	0.017	0.001	Sp
GalC	VCC 1931	12h42m40.7s	+13d16m01s	Irr[f]					N/A
				RSCG 86					
GalA	NGC 7720 NED01	23h38m29.4s	+27d01m53s	N/A	0.700	0.001	-0.018	0.017	E; St
GalB	NGC 7720 NED02	23h38m29.5s	+27d02m05s	E[q]					N/A
GalC	IC 5342	23h38m38.8s	+27d00m41s	E[f]	0.400	0.002	-0.051	0.114	E; St; x
GalD	2MASX J23383626+2701467	23h38m36.2s	+27d01m47s	S0[q]	1.169	0.001	-0.066	0.055	E; x
				HCG 2					
GalA	UGC 00312	00h31m23.9s	+08d28m01s	S[f]	3.919	0.002	0.133	0.005	STB
GalB	UGC 00312 NOTES01	00h31m18.8s	+08d28m29s	S[f]	4.536	0.002	0.304	0.006	U/L
GalC	UGC 00314	00h31m29.4s	+08d24m02s	S[f]	3.366	0.01	-0.002	0.03	Sp; Sp/L; x
				HCG 4					
GalA	ESO 540- G 001	00h34m13.8s	-21d26m21s	S[f] ; Seyfert 2[h]	4.213	0.002	0.377	0.005	STB
GalB	ESO 540- G 002	00h34m14.0s	-21d28m12s	S[f]	3.386	0.005	0.094	0.005	Sp/L
GalC	2MASX J00341549-2125030	00h34m15.5s	-21d25m03s	S0[f]	1.032	0.002	0.026	0.077	E
GalD	KUG 0031-217B	00h34m16.8s	-21d28m40s	E[f]	3.990	0.001	0.109	0.005	STB;U/L
				HCG 7					

TABLE 2—*Continued*

Member ID[a]	Galaxy Name	RA(J2000)	Dec (J2000)	NED Classification[b]	w2-w3[c]	σ_{w2-w3}	w1-w2[d]	σ_{w1-w2}	Classification[e]
GalA	NGC 0192	00h39m13.4s	+00d51m52s	S[f]	3.603	0.003	0.160	0.003	Sp/L
GalB	NGC 0196	00h39m17.8s	+00d54m46s	SB0[f]	0.563	0.004	-0.076	0.035	E; St; x
GalC	NGC 0201	00h39m34.8s	+00d51m36s	SAB[f]	3.818	0.0009	0.040	0.005	L
GalD	NGC 0197	00h39m18.8s	+00d53m31s	SB0[f]	3.224	0.004	0.007	0.014	Sp; Sp/L
				HCG 15					
GalA	UGC 01624	02h07m53.1s	+02d10m03s	S0[f]	1.491	0.001	-0.066	0.009	Sp; x
GalB	UGC 01617	02h07m34.1s	+02d06m55s	S0[f]	0.511	0.001	-0.052	0.067	St
GalC	UGC 01620	02h07m39.8s	+02d08m59s	S0[f]	0.535	0.001	-0.710	0.054	St; x
GalD	UGC 01618	02h07m37.5s	+02d10m50s	S0[f]	1.723	0.001	0.082	0.021	Sp
GalE	ARK 074	02h07m25.3s	+02d06m58s	S0[f]	1.180	0.001	-0.067	0.061	E; x
GalF	UGC 01618 NOTES01	02h07m37.8s	+02d11m25s	N/A	3.545	0.009	0.088	0.012	Sp/L
				HCG 16					
GalA	NGC 0835	02h09m24.6s	-10d08m09s	SAB[f] ; Seyfert 2[g]	3.792	0.003	0.217	0.005	STB
GalB	NGC 0833	02h09m20.8s	-10d07m59s	S[f] ; LINER[g]	1.465	0.002	0.001	0.002	Sp
GalC	NGC 0838	02h09m38.5s	-10d08m48s	SA[f] ; LIRG[i]	4.486	0.002	0.380	0.005	U/L
GalD	NGC 0839	02h09m42.9s	-10d11m03s	S0[f] ; LIRG[i]	4.430	0.002	0.642	0.005	U/L
				HCG 22					
GalA	NGC 1199	03h03m38.4s	-15d36m48s	E3[f]	0.634	0.003	-0.036	0.006	E; St
GalB	NGC 1190	03h03m26.1s	-15d39m43s	S0[f]	0.651	0.0009	-0.084	0.158	E; St; x
GalC	NGC 1189	03h03m24.5s	-15d37m24s	SB[f]	2.844	0.004	-0.011	0.026	Sp
				HCG 25					
GalA	UGC 02690	3h20m42.9s	-01d06m31s	SA[f]	4.027	0.002	0.142	0.005	STB; U/L
GalB	UGC 02691 NED01	3h20m45.4s	-01d02m41s	N/A	1.933	0.003	-0.026	0.008	Sp
GalD	CGCG 390-067	3h20m38.5s	-01d02m06s	SA[f]	0.712	0.002	-0.077	0.204	E; St; x
GalF	UGC 02691 NED02	3h20m45.3s	-01d03m14s	S0[f]	0.983	0.003	-0.042	0.198	E; x
				HCG 31					
GalA	NGC 1741 NED04	05h01m38.7s	-04d15m34s	Wolf-Rayet Galaxy[l]	4.921	0.001	0.609	0.008	U/L
GalB	NGC 1741 NED01	05h01m36.2s	-04d15m43s	SB[f]	3.181	0.057	0.024	0.113	Sp; Sp/L
GalC	NGC 1741 NED03	05h01m37.7s	-04d15m28s	SB[f] ; Starburst[j]	4.910	0.001	0.609	0.008	N/A
GalE	HCG 031E	05h01m37.5s	-04d15m57s	SB[f] ; Starburst[j]	4.284	0.058	-0.076	0.01	L
GalF	GALEX 2732886767084503642	5h01m40.0s	-04d16m22s	N/A					N/A
GalG	IC 0399	05h01m44.0s	-04d17m20s	IAB[f]	3.261	0.005	-0.025	0.008	Sp
GalQ	HCG 031Q	05h01m38.3s	-04d13m21s	N/A					N/A

Table 2—*Continued*

Member ID[a]	Galaxy Name	RA(J2000)	Dec (J2000)	NED Classification[b]	w2-w3[c]	σ_{w2-w3}	w1-w2[d]	σ_{w1-w2}	Classification[e]
				HCG 37					
GalA	NGC 2783	09h13m39.4s	+29d59m35s	E[f]	0.059	0.004	-0.046	0.025	St
GalB	NGC 2783B	09h13m33.1s	+30d00m01s	Sb[f]	3.001	0.001	0.176	0.001	Sp;Sp/L
GalC	MCG +05-22-020	09h13m37.3s	+29d59m58s	S[f]	1.940	0.002	0.092	0.052	Sp
GalD	MCG +05-22-016	09h13m33.8s	+30d00m57s	S0[f]	3.263	0.055	-0.043	0.109	Sp; x
GalE	MCG +05-22-018	09h13m34.0s	+30d02m23s	S[f]	2.014	0.007	-0.065	0.099	Sp; x
				HCG 38					
GalA	CGCG 062-036	09h27m34.6s	12d16m09s	S[f]	3.826	0.002	0.167	0.003	STB
GalB	UGC 05044 NED01	09h27m43.5s	12d17m15s	S[f]	3.988	0.004	0.227	0.004	STB
GalC	UGC 05044 NED02	09h27m44.5s	12d17m16s	S[f]	4.045	0.0009	0.190	0.002	STB
				HCG 47					
GalA	UGC 05644	0h25m46.2s	+13d43m01s	SA[f]	2.497	0.001	-0.044	0.008	Sp
GalB	MCG +02-27-013	0h25m48.6s	+13d43m41s	S0[f]	0.634	0.001	-0.078	0.103	E; St; x
GalC	MCG +02-27-015	0h25m49.0s	+13d45m11s	N/A	3.258	0.005	0.064	0.017	Sp/L
GalD	MCG +02-27-014	0h25m47.7s	+13d44m57s	N/A	2.646	0.007	0.108	0.067	Sp
				HCG 54					
GalA	IC 0700 NED02	11h29m15.3s	+20d34m59s	N/A	2.787	0.009	0.069	0.05	Sp
GalB	IC 0700 NED01	11h29m14.1s	+20d34m52s	S[f]	4.262	0.01	0.421	0.007 STB	
GalC	IC 0700 NED03	11h29m16.4s	+20d35m08s	N/A	3.419	0.023	0.230	0.047	Sp/L
GalD	IC 0700 NED04	11h29m16.7s	+20d35m16s	N/A	3.419	0.023	0.230	0.047	N/A
				HCG 56					
GalA	UGC 06527 NOTES02	11h32m46.7s	+52d56m27s	S[f]	3.050	0.062	-0.020	0.003	Sp
GalB	UGC 06527 NED03	11h32m40.2s	+52d57m01s	Seyfert 1[g]	3.127	0.002	0.869	0.007	Sy
GalC	UGC 06527 NED02	11h32m36.7s	+52d56m52s	S0[f]	1.168	0.001	0.003	0.04	E
GalD	UGC 06527 NED01	11h32m35.3s	+52d56m50s	SA[f]	3.614	0.0009	0.099	0.003	Sp/L
GalE	UGC 06527 NOTES01	11h32m32.8s	+52d56m21s	SB0[f]	3.141	0.002	0.033	0.008	Sp
				HCG 57					
GalA	NGC 3753	11h37m53.9s	+21d58m53s	Sab[f]	1.621	0.003	0.009	0.006	Sp
GalB	NGC 3746	11h37m43.6s	+22d00m35s	SB[f]	1.434	0.002	-0.070	0.039	Sp; x
GalC	NGC 3750	11h37m51.6s	+21d58m27s	SAB0[f]	0.520	0.002	-0.141	0.082	St; x
GalD	NGC 3754	11h37m54.9s	+21d59m08s	SB0[f]	3.145	0.001	-0.010	0.002	Sp
GalE	NGC 3748	11h37m49.0s	+22d01m34s	SB0[f]	1.571	0.008	0.002	-0.046	Sp; x
GalF	NGC 3751	11h37m53.8s	+21d56m11s	S0[f]	0.764	0.002	-0.094	0.125	E; St; x
GalG	NGC 3745	11h37m44.4s	+22d01m17s	SB0[f]	0.665	0.0009	-0.120	0.144	St; x

Table 2—*Continued*

Member ID[a]	Galaxy Name	RA(J2000)	Dec (J2000)	NED Classification[b]	w2-w3[c]	σ_{w2-w3}	w1-w2[d]	σ_{w1-w2}	Classification[e]
GalH	2MASX J11375047+2200450	11h37m50.5s	+22d00m45s	N/A	2.772	0.008	0.068	0.068	Sp
				HCG 59					
GalA	IC 0737	11h48m27.5s	+12d43m39s	E[f]	4.150	0.002	0.558	0.006	STB
GalB	IC 0736	11h48m20.1s	12d43m00s	S0[f]					N/A
GalC	KUG 1145+129	1h48m32.4s	+12d42m19s	S[f]	3.013	0.013	0.117	0.051	Sp
GalD	KUG 1145+130	1h48m30.6s	+12d43m47s	S[f]	2.997	0.045	0.072	0.175	Sp
				HCG 61					
GalA	NGC 4169	12h12m18.8s	+29d10m46s	S0[f] ; Seyfert 2[g]	1.232	0.005	0.005	0.003	E
GalC	NGC 4175	12h12m31.0s	+29d10m06s	S[f]	3.576	0.002	0.161	0.002	STB
GalD	NGC 4174	12h12m26.9s	+29d08m57s	S[f]	3.614	0.008	0.077	0.008	E; x
				HCG 71					
H71A	NGC 5008	14h10m57.2s	+25d29m50s	Scd[f]	2.770	0.002	0.073	0.002	Sp
H71B	IC 4382	14h11m02.5s	+25d31m10s	S[f]	3.576	0.002	0.161	0.002	Sp/L
H71C	KUG 1408+257	14h11m05.1s	+25d28m58s	S[f]	3.614	0.008	0.077	0.008	Sp/L
				HCG 79					
GalA	NGC 6027a	15h59m11.1s	+20d45m17s	Sa[f]	2.770	0.002	0.073	0.002	Sp
GalB	NGC 6027	15h59m12.5s	+20d45m48s	S0[f]	2.351	0.002	0.028	0.002	Sp
GalC	NGC 6027b	15h59m10.8s	+20d45m44s	S0[f]	0.507	0.001	0.087	0.175	E; St
GalD	NGC 6027c	15h59m11.8s	+20d44m49s	SB[f]	3.164	0.015	0.041	0.043	Sp
				HCG 92					
GalA	NGC 7320	22h36m03.4s	+33d56m53s	SA[f]	2.662	0.004	0.009	0.014	Sp
GalB	NGC 7318B	22h35m58.4s	+33d57m57s	SB[f]	0.712	0.001	0.051	0.033	E
GalC	NGC 7319	22h36m03.5s	+33d58m33s	SB[f] ; Seyfert 2[g]	3.163	0.001	0.920	0.009	Q
GalD	NGC 7318A	22h35m56.7s	+33d57m56s	E2[f]	0.590	0.001	0.920	0.006	Sp
GalE	NGC 7317	22h35m51.9s	33d56m42s	N/A	0.465	0.004	0.062	0.049	E; St
				HCG 96					
GalA	NGC 7674	23h27m56.7s	+08d46m45s	SA[f] ; LIRG[i] ; Seyfert 2[k]	3.483	0.002	1.165	0.006	Q
GalB	NGC 7675	23h28m05.9s	+08d46m07s	SAB0[f]	0.654	0.002	-0.116	0.051	St; x
GalC	NGC 7674A	23h27m58.8s	+08d46m58s	S[f]	3.552	0.0009	0.117	0.004	Sp/L
GalD	HCG 096D	23h28m00.2s	+08d46m02s	N/A	4.083	0.012	0.209	0.002	STB
				HCG 97					

Table 2—*Continued*

Member ID[a]	Galaxy Name	RA(J2000)	Dec (J2000)	NED Classification[b]	w2-w3[c]	σ_{w2-w3}	w1-w2[d]	σ_{w1-w2}	Classification[e]
GalA	IC 5357	23h47m23.0s	-02d18m02s	SAB0[f]	0.454	0.0009	-0.107	0.064	St; x
GalB	IC 5359	23h47m37.8s	-02d19m00s	S[f]	2.821	0.002	-0.076	0.01	Sp
GalC	IC 5356	23h47m23.8s	-02d21m04s	S[f]	0.391	0.002	-0.087	0.115	St
GalD	IC 5351	23h47m18.9s	-02d18m49s	E[f]	0.092	0.002	-0.069	0.049	St; x
GalE	IC 5352	23h47m19.9s	-02d16m50s	N/A					N/A
				HCG 100					
GalA	NGC 7803	00h01m20.0s	+13d06m41s	S0[f]	3.217	0.002	0.113	0.007	Sp/L
GalB	MRK 0934	00h01m26.0s	+13d06m47s	S[f]	3.749	0.001	0.140	0.003	STB
GalC	KUG 2358+128A	00h01m13.4s	+13d08m39s	S[f]	3.301	0.006	0.102	0.013	Sp/L
GalD	MCG +02-01-010	00h01m15.0s	+13d06m45s	N/A	2.883	0.018	0.157	0.087	Sp

[a] The original catalogs (e.g.HCG) sometimes included galaxies that were mislabeled as part of the CG. The identification presented here indicates the galaxy member in the CG based on a magnitude limited system in accordance to the original labeling from the catalogs.

[b] Classifications of the galaxies from NASA/IPAC Extragalactic Database (NED) using the standard symbols for the classification of galaxies. Individual references listed.

[c] WISE colors w2 and w3 corresponding to the magnitude of 4.6 and 12 μm respectively. This column corresponds to the 'x' axis on the WISE color-color graphs.

[d] WISE colors w1 and w2 corresponding to magnitude of 3.4 and 4.6 μm respectively. This column corresponds to the 'y' axis on the WISE color-color graphs.

[e] Classification of the galaxies based on the results of this paper. For cases of multiple classifications based on the error, the possible classifications are separated by a ';' with no preference for the order. (See Table Note for the symbol legend.)

[f] de Vaucouleurs et al. (1991)

[g] Véron-Cetty & Véron (2006)

[h] Panessa & Bassani (2002)

[i] Sanders et al. (2003)

[j] Balzano (1983)

[k] Osterbrock & Martel (1993)

[l] Conti (1991)

[m] Karachentseva et al. (1979)

[n] Zwicky et al. (1965)

[o] Nilson (1973)

[p] Arakelian (1975)

[q]Hardcastle et al. (2005)

NOTE.—The symbols used for the identification of the galaxies from this paper are as follows: U/L, ULIRG/LINER; Q, QSO; St, Stars; E, Elliptical; Sp, Spiral; STB, Starburst; Sy, Seyfert; L, LIRG; Sp/L, Spiral/LIRG; x, no identification. The classifications are from the regions on the WISE color-color diagram, Figure 6

REFERENCES

Arakelian, M. A. 1975, SoByu, 47, 3A

Arp, H. 1973 ApJ, 185, 797A

Balzano, V. A 1983 ApJ, 268, 602B

Barton, E., Geller, M., Ramella, M., Marzke, R. O., & da Costa, L. N. 1996 ApJ, 112, 871B

Barnes, J. 1984 MNRAS, 208, 873B

Barnes, J. E. 1989 Nature, 338, 123

Bode, P. W., Cohn, H. N., & Lugger, P. M. 1993 ApJ, 416, 17B

Butterfield et al. in progress

Carnevali, P., Cavaliere, A., & Santangelo, P. 1981 ApJ, 249, 449

Cavaliere, A., Santangelo, P., Tarquini, G., & Vittorio, N. 1983, in Clustering in the Universe, edited by D. Gerbal and A. Mazure (Éditions Frontières, Gif-sur-Yvette), p.25

Conti, P. S. 1991 ApJ, 377, 115C

de Vaucouleurs et al. 1991, Third Reference Catalogue of Bright Galaxies. Volume I: Explanations and references. Volume II: Data for galaxies between 0^h and 12^h. Volume III: Data for galaxies between 12^h and 24^h (New York, NY:Springer)

Governato, F., Tozzi, R., & Cavaliere, A. 1995 ApJ, 458, 18

Hardcastle, M. J., Sakelliou, I., & Worrall, D. M. 2005 MNRAS, 359, 1007H

Hickson, P., Richstone, D. O., & Turner, E. L. 1977 ApJ, 213, 323H

Hickson, P. 1982 ApJ, 255, 382H

Hickson, P. 1984 ASSL, 111, 367H

Hickson, P. & Rood, H. J. 1988 ApJ, 331L, 69H

Hickson, P., Mendes de Oliveira, C., Huchra, J. P., & Palumbo, G. G 1992 ApJ, 399, 353H

Hickson, P. 1993 ApJ, 29, 1H

Hickson, P. 1997 ARA&A, 117, 39A

Hogg, D. W., Blanton, M. R., Brinchmann, J. et al. 2004 ApJ, 601L, 29H

Johnson, K. E., Hibbard, J. E., Gallagher, S. C., Charlton, J. C., Hornshemeier, A. E., Jarrett, T. H., & Reines, A. E. 2007 AJ, 134, 1522

Karachentseva, V. E., Karachentesev, I. K., & Shcherbanovsky, A. L. 1979 AISAO, 11, 3K

Konstantopoulos, I. S., Gallagher, S. C., Fedotov, K., et al. 2010 ApJ, 723, 197

Kindl, E. 1990 PhDT, 20K

Malykh, S. A. & Orlov, V. V. 1986, Astrofizika, 24, 445M

Mamon, G. A. 1986 ApJ, 307, 426

Menon, T. K. 1995 MNRAS, 274, 845M

Nilson, P. 1973 Uppsala General Catalogue of Galaxies, Acta Universitatis Upsalienis, Nova Regiae Societatis Upsaliensis, Series v: a Vol.

Osterbrock, D. E. & Martel, A. 1993 ApJ, 414 552O

Panessa, F. & Bassani, L 2002 A&A, 394, 435P

Pompei, E. & Iovino, A. 2012 A&A, 539, A106

Rood, H. J. & Williams, B. A. 1989 ApJ, 339, 772R

Rose, J. A. 1977 ApJ, 231, 320R

Rubin, V. C., Hunter, D. A., & Ford, W. K., Jr. 1991 ApJS, 76, 153R

Sanders, D. B., Mazzarella, J. M., Kim, D.-C., et al. 2003 AJ, 126, 1607S

Smolčić, V. 2009 ApJ, 699L, 43S

Tzanavaris, P., Hornschemeier, A. E., Gallagher, S. C., et al. 2010 ApJ, 716, 556

Verdes-Montenegro, L., Yun, M. S., Williams, B. A., et al. 2000 Astronomical Society of the Pacific Conference Series, 209, 167V

Verdes-Montenegro, L., Yun, M. S., Williams, B. A., et al. 2001 A&A, 377, 812V

Véron-Cetty, M. -P. & Véron, P. 2006 A&A, 455, 773V

Walker, L. M., Johnson, K. E., Gallagher, S. C., et al. 2010 AJ, 140, 1254

Walker, L. M., Johnson, K. E., Gallagher, S. C., et al. 2012 AJ, 143, 69W

Williams, B. A. & Rood, H. J. 1987 ApJS, 63, 265W

Wright, E. L., Eisenhardt, P. R. M., Mainzer, A. K., et al. 2010 AJ, 140, 1868

Zwicky, F., Karpowica, M., & Kowal, C. T. 1965 Catalogue of Galaxies and of Clusters of Galaxies", Volume V Pasadena: California Institute of Technology

This 2-column preprint was prepared with the AAS LaTeX macros v5.2.